COMPARATIVE STUDY ON PROPERTIES OF NANOSTRUCTURED TITANIA SYNTHESIZED BY COLLOIDAL AND POLYMERIC SOL-GEL ROUTES

V. Tajer-Kajinebaf[1], H. Sarpoolaky[1,*] and T. Mohammadi[2]

* *hsarpoolaky@iust.ac.ir*

Received: October 2012 **Accepted: January 2013**

[1] School of Metallurgy and Materials Engineering, Iran University of Science & Technology ,Tehran, Iran.
[2] Research Laboratory for Separation Processes, Faculty of Chemical Engineering, Iran University of Science and Technology, Tehran, Iran.

Downloaded from ijmse.iust.ac.ir at 5:31 IRDT on Sunday June 24th 2018

Abstract:*Nanostructured titania was synthesized by colloidal and polymeric sol-gel routes. Stable colloidal and polymeric titania sols were prepared by adjusting the proper values of the acid/alkoxide and the water/alkoxide molar ratios. The properties of sols were determined by dynamic light scattering technique and synthesized titania was characterized by thermogravimetry and differential thermal analysis, X-ray diffraction, Fourier transform infrared spectroscopy, optical microscopy and field emission scanning electron microscopy. The results showed particle size distribution of colloidal sol 10-50 nm compared to polymeric one which was 0.5-2 nm. Phase analysis of the colloidal sample revealed anatase as the major phase up to 550 °C, while the polymeric route resulted only anatase phase up to 750 °C. On the basis of results, titania prepared by the polymeric route showed better thermal stability against phase transformation than the sample prepared by the colloidal route. Also, microstructural studies showed that titania nanopowder can be produced by both sol-gel routes.*

Keywords: *Nanostructured Titania; Colloidal sol; Polymeric sol; TiO_2*

1. INTRODUCTION

Nowadays nanostructured titania has found increasingly attention in science and research interest due to its potential applications such as photovoltaic [1-3], photocatalytic [4-6], electrochromic devices [4-7], sensing applications and etc. [4,8]. Among the different synthesis methods, sol-gel technique has shown promising results because of the relative simplicity of the procedure and the almost unlimited number of possibilities for the formation of materials with improved or new properties [9] such as homogeneous multi-component systems [10], mesoporous and macroporous materials, nanopowders, fibers, thin films and etc. [11]. The sol-gel method which is a versatile process used in making various ceramic materials is a general name for a process that converts a colloidal or polymeric "solution" (sol), to a gelatinous substance (gel) [9]. Generally the sol–gel process can be divided into two main types: the colloidal (particulate) and the polymeric sol–gel routes [9,12]. In sol-gel process a metal alkoxide or inorganic salt is hydrolyzed and a simultaneous condensation reaction occurs to form colloidal or polymeric sols [12]. The so-called colloidal route is based on the formation of colloids in aqueous media, where the particles are prevented from agglomeration by mutual repulsion of similar charges at the particle surface [9]. In this method, the hydrolysis and condensation reactions are fast, compared with the polymeric sol route. The rapid condensation reaction in the colloidal sol route causes particulate growth and/or the formation of precipitates. Colloidal sols can be obtained by the precise control of reaction conditions and/or the peptization of the precipitate by adding acid [12]. While in the polymeric route, metal-organic precursors are reacted in alcoholic media, where the polymeric particles remain separated because of their small size [9]. In this route, the hydrolysis reaction is slower and is typically achieved by adding a small amount of water, resulting in a partially hydrolyzed alkoxide leading to the formation of a linear inorganic polymer. Through the subsequent gellation process, polymeric sols form a gel network [12]. Colloidal sols are

Downloaded from ijmse.iust.ac.ir at 5:31 IRDT on Sunday June 24th 2018

generally used for the production of crystalline [9,12] and mesoporous materials, while by polymeric sols, amorphous and microporous materials may be formed [9]. Fig. 1 shows schematic diagram of synthesis processes by colloidal and polymeric sol-gel routes.

Nanostructured titania is mostly produced by sol-gel technique [14-20]. The sol-gel chemistry of transition metal alkoxide as titanium is complex, because transition metal precursors are highly reactive due to have a low electronegativity and can exhibit various coordination numbers [9]. Metal alkoxides are popular precursors because they react readily with water [21]. Many researchers used titanium tetraisopropoxide (Ti(OPr)4) to produce nanostructured titania by colloidal or polymeric sol-gel routes [18,22-29].

In colloidal route, hydrolysis-condensation reactions can be written as Eq. (1,2):

$$Ti(OPr)_4 + xH_2O \rightarrow Ti(OH)_4 + 4PrOH + (x-4)H_2O \quad \text{(hydrolysis)} \quad (1)$$

$$Ti(OH)_4 + Ti(OH)_4 \rightarrow (HO)_3TiOTi(OH)_3 + H2O \quad \text{(condensation)} \quad (2)$$

$(x \geq 4)$

After peptization with acid and reflux, the result is a clear blue stable titania sol.

In polymeric route that produces transparent sol, hydrolysis-condensation reactions can be written as Eq. (3,4):

$$Ti(OPr)_4 + xH_2O \rightarrow Ti(OPr)_4\text{-}x(OH)x + xPrOH \quad \text{(hydrolysis)} \quad (3)$$

$$Ti(OPr)_4 + Ti(OPr)_{4-x}(OH)_x \rightarrow (PrO)_{4-x}TiOTi(OPr)_{4-x} + xPrOH \quad \text{(condensation)} \quad (4)$$

$(x < 4)$

The prepared products precisely are heated to remove hydroxyl and organic groups and finally TiO_2 will be synthesized after calcination.

The present study focuses on the comparison of titania colloidal and polymeric sols, as well as the properties of nanostruructured titanaia synthesized by these routes.

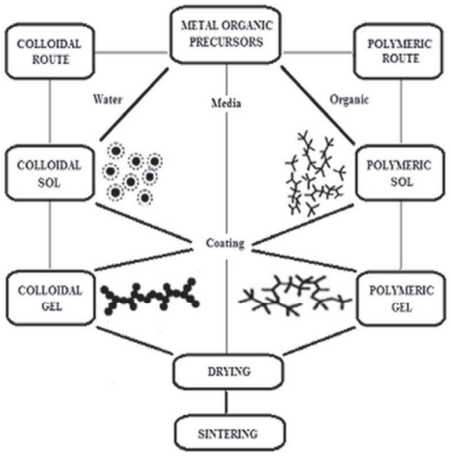

Fig. 1. Schematic diagram of synthesis processes by colloidal and polymeric sol-gel routes [13]..

2. EXPERIMENTAL PROCEDURES

2. 1. Materials

Titanium tetraisopropoxide (TTIP, $Ti(OC_3H_7)_4$) (Merck, 821895), isopropanol (IPA, C_3H_7OH) (Merck, 109634), hydrochloric acid (37% solution) (Merck, 100317) and deionized water were used as received without further purification as raw materials for synthesis of colloidal and polymeric titania sols.

2. 2. Preparation of Samples

2. 2. 1. Colloidal method

Colloidal titania sol was prepared by hydrolysis of titanium tetraisopropoxide via the addition of an excess H_2O ($[H_2O]/[Ti] > 4$). A solution of TTIP in isopropanol (0.45 mol/lit) was added dropwise to a solution of water in isopropanol (4.5 mol/lit) while stirring at high speed. Then the alcohol was removed from the solution by rotary system and the washed product was dispersed in water to achieve to Ti concentration of 0.4 mol/lit. The solution was peptized with acid by adjusted pH to 1.5 and was refluxed at about 75 °C for 20 hr. The result was a semi-opaque titania dispersion. Then to break

Downloaded from ijmse.iust.ac.ir at 5:31 IRDT on Sunday June 24th 2018

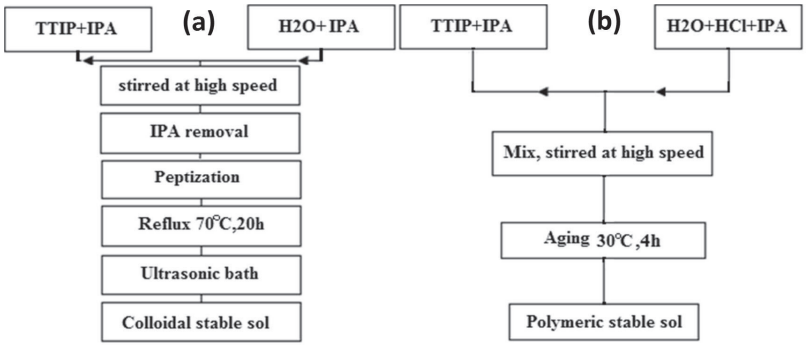

Fig. 2. Preparation processes of titania sols by the a) colloidal and b) polymeric routes.

the weakly agglomerated particles, the sol was poured in beaker glass and subsequently held for 1 hr in an ultrasonic bath. Finally a clear blue stable sol was obtained by this method.

2. 2. 2. Polymeric Method

Polymeric titania sol was obtained by hydrolysis of titanium tetraisopropoxide by addition of a less than equivalent amount of H_2O ($[H_2O]/[Ti] < 4$) in order to obtain a precipitate free polymeric sol. A solution of water and hydrochloric acid as a catalyst in isopropanol was added dropwise to a solution of TTIP in isopropanol during high speed stirring. The molar ratio for TTIP:IPA:H_2O:HCl of the final sol was 1:31:0.8:0.23, respectively. Stirring was continued for 4 hr to get a stabilized sol. So, the final product was a stable transparent titania sol.

The preparation processes of the colloidal and polymeric sols are shown in Fig. 2 (a,b).

For gel preparation, the colloidal and polymeric sols were dried at room temperature for 48 hr and in oven at 110 °C for 24 hr. Then resultant gels were subsequently calcined at 400, 550, 650, 750 and 850 °C in air for 1 hr with a heating rate of 1 °C/min.

Also, to compare resultant coatings of the colloidal and polymeric sols, TiO_2 films were deposited by dip-coating from both sols on glass slides. The coatings were treated in air at 450 °C for 1 hr using heating rate of 1 °C/min.

2. 3. Characterizations

Particle size distribution of the prepared sols was determined by dynamic light scattering technique (DLS, Malvern, UK, ZS3600). Thermal properties of the dried gels were characterized by differential thermal and thermogravimetric analysis (DTA-TG, PERKINELMER) in a nitrogen flow with a heating rate of 7.5 °C/min up to 900 °C. The phase composition and the average crystallite size of the samples were identified using X-ray diffraction technique with Cu Kα wavelength at 30 mA and 40 kV (XRD, Jeol JDX-8030). Infrared measurements were performed using FTIR spectrometer (Bruker, Tensor 27) at room temperature on sample wafers consisting of 100 mg dry KBr and about 1 mg sample. Optical microscope (MO, Meiji Techno, ML7100) was used to study the homogeneity and microstructure of the coatings. Also, the morphology of the samples was characterized by field emission scanning electron microscope (FESEM MIRA\\TESCAN) with an accelerating voltage of 20 kV.

3. RESULTS AND DISCUSSION

3. 1. Particle size distribution

Particle size distribution of the colloidal and polymeric sols is shown in Fig. 3.

Results showed particle size of the colloidal and polymeric sols is in the range of 10-50 nm

Downloaded from ijmse.iust.ac.ir at 5:31 IRDT on Sunday June 24th 2018

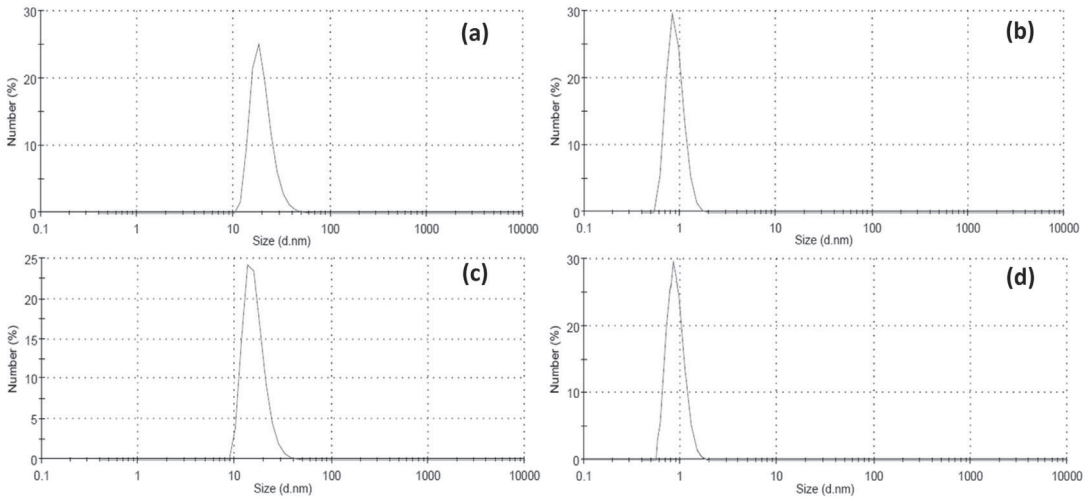

Fig. 3. The particle size distribution determined by the dynamic light scattering technique:
a,b) colloidal and polymeric sols, respectively;
c,d) colloidal and polymeric sols after aging, respectively.

and 0.5-2 nm, respectively. The particle size distribution of the colloidal sample showed a little shift to the smaller size after 50 days aging at room temperature while it has not changed for the polymeric sol within period.

Comparing these curves, it can be seen that the particle size distribution of the colloidal sol is broader and the mean particle size (20 nm) is larger than that of the polymeric sol (0.8 nm). In fact, in colloidal route due to excess of water, hydrolysis occurs faster and leads to the formation of larger particles. Also, stability of the colloidal sol is less than that of polymeric sol due to precipitation of large particles after 50 days aging at room temperature.

In colloidal sol the growth of particles from nuclei proceeds by diffusion of solute precursors into the existing nuclei. Once primary particles are formed, the small ones dissolve, and the product species are incorporated into the large particles, which leads to disappearance of small particles while large particles become bigger. Particle growth can also continue through an aggregation process, the prevention or control of which is often described as sol stability. While in polymeric sol, hydrolysis and condensation reactions carried out under certain carefully controlled conditions may lead to the formation of a three-dimensional network of branched polymers. These polymeric systems grown by random processes are fractal objects and can be represented by a mass fractal dimension (Df) that relates the mass m to the radius r of the sol particle via $m \propto r^{Df}$ [9].

3. 2. Thermal analysis Properties

The differential thermal and thermogravimetric analysis of the colloidal and polymeric samples (dried gels) are presented in Fig. 4 (a,b).

The thermogravimetric curve of the colloidal samples (Fig. 4a) follows 19% weight loss during two steps. The first step extends up to about 100 °C that is attributed to the removal of adsorbed water corresponding to endotherm peak [24,30,31]. The second step extends up to 420 °C and shows the expulsion of organics and the dehydroxylation of $Ti(OH)_4$. The dehydroxylation step is along with TiO_2 phase transition according to exotherm peaks at 150 and 300 °C. The former corresponds to TiO_2 phase transition from amorphous to anatase and the latter could be due to phase transition from anatase to rutile. Finally the weight loss ends at about 400 °C which is minimum calcination temperature for complete removal of the organic molecules.

The thermogravimetric curve of the polymeric sample (Fig. 4b) follows 45% weight loss during three steps. The first step that extends up to 200 °C can be attributed to the removal of alcohol and

Downloaded from ijmse.iust.ac.ir at 5:31 IRDT on Sunday June 24th 2018

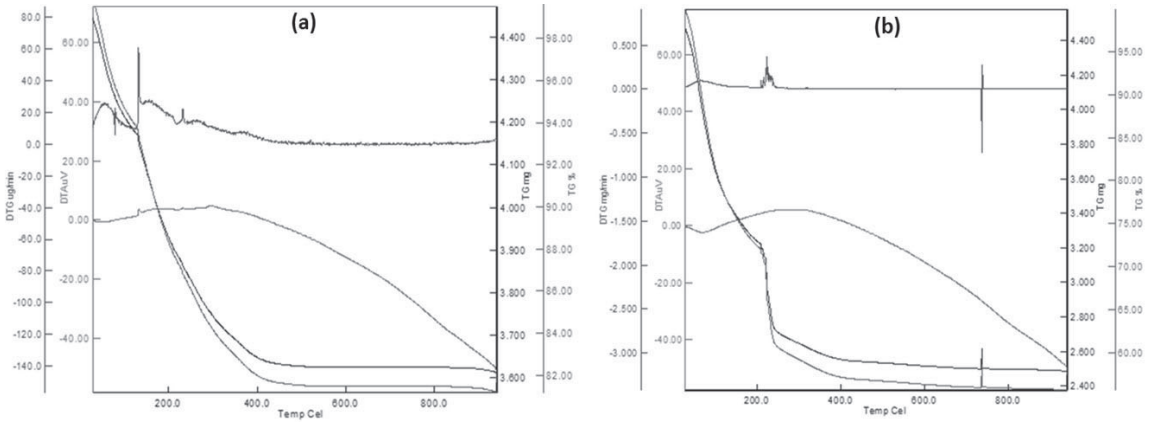

Fig. 4. The differential thermal and thermogravimetric analysis of the a) colloidal and b) polymeric samples.

adsorbed water [9]. The second step to 250 °C corresponds to removal of isopropoxy groups (-OC_3H_7) [9] and the third step that extends up to 400 °C can be attributed to the dehydroxylation of $Ti(OH)_4$. The board exotherm peak corresponding to the third step is attributed to TiO_2 phase transition from amorphous to anatase and the weight loss beyond 400 °C is negligible that is in agreement with the literature [9]. No significant thermal effects of the transformation of the anatase into the rutile phase are detected up to higher temperature.

Comparing themogravimetric curves, it can be seen that weight loss of the polymeric sample is more than colloidal one due to removal of isopropoxy groups that can be shown according to:

Also, comparing differential thermal analysis curves shows that anatase-to-rutile phase transition is shifted to higher temperature in the sample prepared by polymeric route.

3. 3. Structural properties

The XRD patterns of the colloidal and polymeric gels calcined at various temperatures are shown in Fig. 5. The strongest peaks of anatase and rutile are located at 2θ = 25.3 ° (101) and 27.4 ° (110), respectively [32].

According to Fig. 5a, anatase peaks in the dried colloidal gel become sharper by increasing calcination temperature. This means that in the colloidal route, anatase phase formed even before calcination while in the polymeric route, no crystalline peak is seen in the dried state. Hence, phase structure of the colloidal gel (without calcination) is anatase; while it is amorphous for the polymeric one. Also the XRD patterns of the colloidal samples indicate anatase as major phase to 550 °C that by increasing temperature until reaching 850 °C, these peaks are gradually resolved and rutile peaks are completed. Phase analysis of the polymeric samples shows purely anatase phase at entire calcination temperatures except 850 °C. The results show that in polymeric route anatase-to-rutile phase transition delays up to 750 °C that can be attributed to remain organic groups even at high temperature according to TG curve (Fig. 4b).

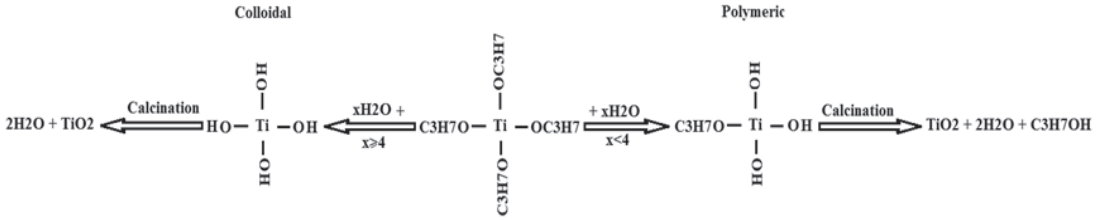

Downloaded from ijmse.iust.ac.ir at 5:31 IRDT on Sunday June 24th 2018

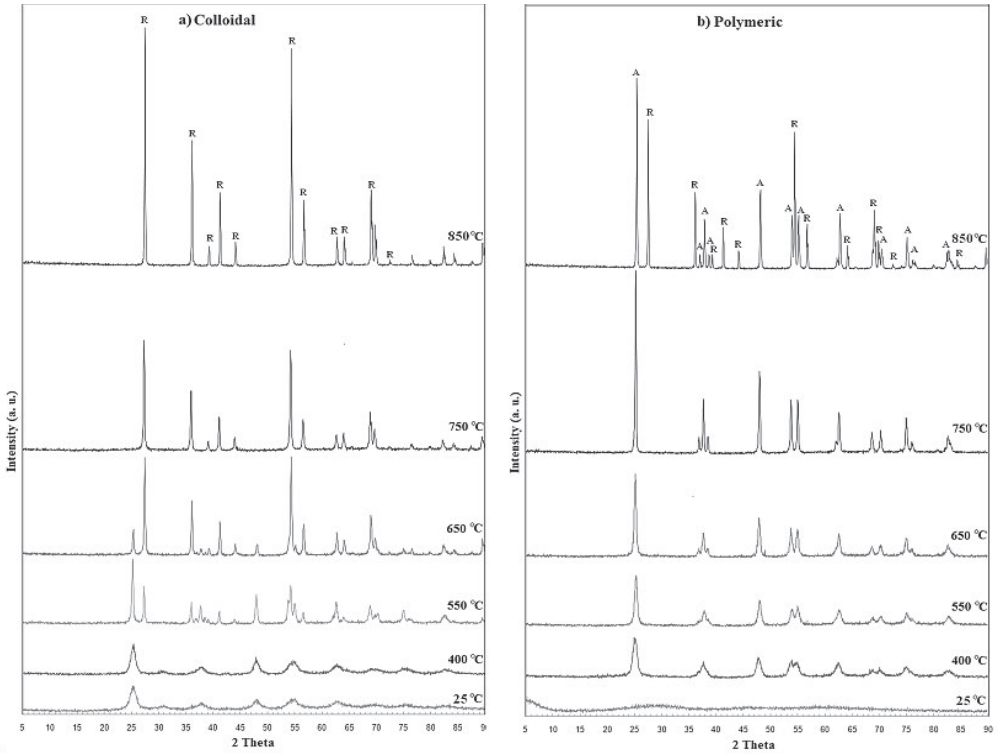

Fig. 5. XRD patterns of the a) colloidal and b) polymeric gels calcined at various temperatures.

The average crystallite size (L) was calculated from the line broadening of X-ray diffraction peak using the Scherrer's equation as expressed by Eq. (5):

$$L=K\lambda/\beta\cos\theta \quad (5)$$

where K is the Scherrer constant usually taken as 0.89, λ is the wavelength of the X-ray radiation (0.15418 nm for Cu Kα), and β is full width half maximum (FWHM) of diffraction peak measured at 2θ [22,33]. The FWHM value was extracted from the XRD pattern fitted using the X'Pert HighScore software. Also, the rutile weight ratio (WR) was estimated from XRD intensity data by using Eq. (6):

$$WR = [1 + 0.8IA/IR]^{-1} \quad (6)$$

Table. 1. XRD results of titania prepared by the colloidal and polymeric routes

Sample	Temp. (°C)	Phase		W_R	Crystallite Size (nm)	
		Major	Minor		Anatase	Rutile
Colloidal	25	Anatase	-	0	8.7	-
	400	Anatase	-	0	8.8	-
	550	Anatase	Rutile	0.43	37.7	37.9
	650	Rutile	Anatase	0.81	37.7	46.2
	750	Rutile	Anatase	0.96	-	37.9
	850	Rutile	-	1	-	59.7
Polymeric	25	Amorph	-	-	-	-
	400	Anatase	-	0	9.6	-
	550	Anatase	-	0	21.8	-
	650	Anatase	-	0	27.6	-
	750	Anatase	-	0	46.0	-
	850	Anatase	Rutile	0.49	59.4	59.7

Downloaded from ijmse.iust.ac.ir at 5:31 IRDT on Sunday June 24th 2018

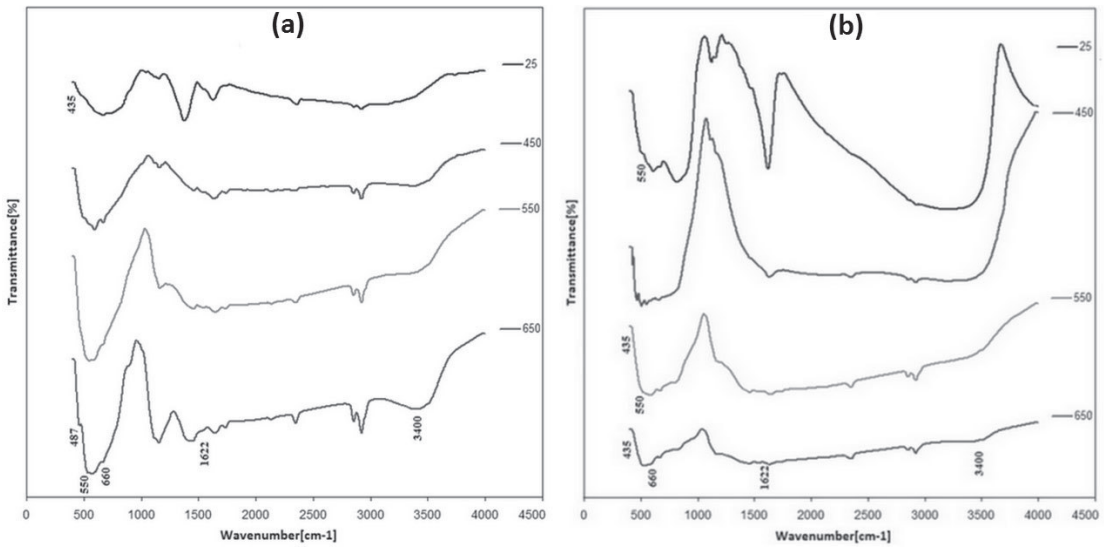

Fig. 6. FTIR absorption spectra of the a) colloidal and b) polymeric samples calcined at different temperatures.

where IA and IR represent X-ray integrated intensity of (101) reflection of anatase and (110) reflection of rutile, respectively [20,33]. The calculated numbers of rutile ratio are also included in Table 1.

So, titania prepared by the polymeric route shows better thermal stability against phase transformation from anatase to rutile.

3. 4. Adsorption Behaviour

The FTIR absorption spectra of the colloidal and polymeric samples calcined at different temperatures are shown in Fig. 6.

The broad band at 2800–3800 cm^{-1} is assigned to O–H for absorbed water molecules [34] and the broad band approximately 3400 cm^{-1} is attributed to the O–H stretching vibration [35,36] of different Ti–OH species. The band at 1622 cm^{-1} is attributed to adsorbed water [35] that is more distinctive in the colloidal samples. The absorption peak at 600–900 cm^{-1} is assigned to Ti-O [37]. Shifu and Gengyu claimed that the band at wave number near to 660 cm^{-1} corresponds to the vibration spectrum of Ti–O [38] that it shifted to about 550 cm^{-1} for the polymeric species. Zhijie Li et al. claimed that Ti–O–Ti vibration appears in the range of 400–600 cm^{-1} as a result of condensation reaction [33]. Also, Djaoued et al. attributed infrared bands in the range of 433–438 cm^{-1} and 489–496 cm^{-1} to anatase and rutile, respectively [27]. According to Fig. 6 the band at 435 cm^{-1} assigned to TiO_2 in anatase phase [39] is more obvious for the polymeric samples.

3. 5. Microstructure and Morphology

To evaluate the properties of the colloidal and polymeric sols for the production of thin film and to compare their behaviour during drying, both sols were deposited on glass substrates in similar conditions with a constant rate of 6 mm/min and immersion time of 30 sec. Fig. 7 shows optical microscope images of TiO_2 films prepared by colloidal and polymeric sols before and after calcination at 450 °C.

The resultant film of the colloidal sol is compact, semi-transparent and crack free (Fig. 7a); while the obtained film of the polymeric sol is transparent and cracked (Fig. 7b). As shown in Fig. 7c, the colloidal film seems without crack after calcination; while cracks in the polymeric film are developed after calcination (Fig. 7d).

SEM images of the colloidal and polymeric sols after drying are shown in Fig. 8. It can be seen that the colloidal sol is agglomerated upon drying while the polymeric specimen is laminated. It seems the removal of alcohol as solvent of the polymeric sol is faster than

Downloaded from ijmse.iust.ac.ir at 5:31 IRDT on Sunday June 24th 2018

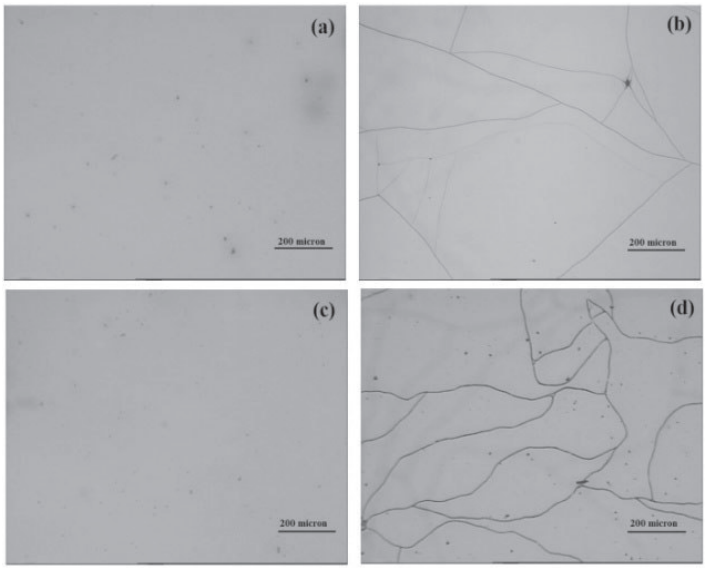

Fig. 7. Microscopic images of TiO2 films deposited on glass substrates of the: (a) colloidal sol before calcination; (b) polymeric sol before calcination; (c) colloidal sol after calcination; (d) polymeric sol after calcination.

evaporation of water as solvent of the colloidal one that can promote crack formation in coatings synthesized by the polymeric route.

As shown in Fig. 9(a,b), the dried colloidal and polymeric gels are formed of spherical particles due to the minimization of the overall surface energy via dissolution and regrowth of monomers during an Ostwald ripening [4]. For particles of nanometric size, the surface energy is an important contribution to the free enthalpy of the dispersion. So, most ultra-divided systems are thermodynamically unstable in suspension and spontaneously evolve in order to decrease the surface area, the growth of particles involving the well-known Ostwald ripening process [39,40]. According to these images, spherical particles of

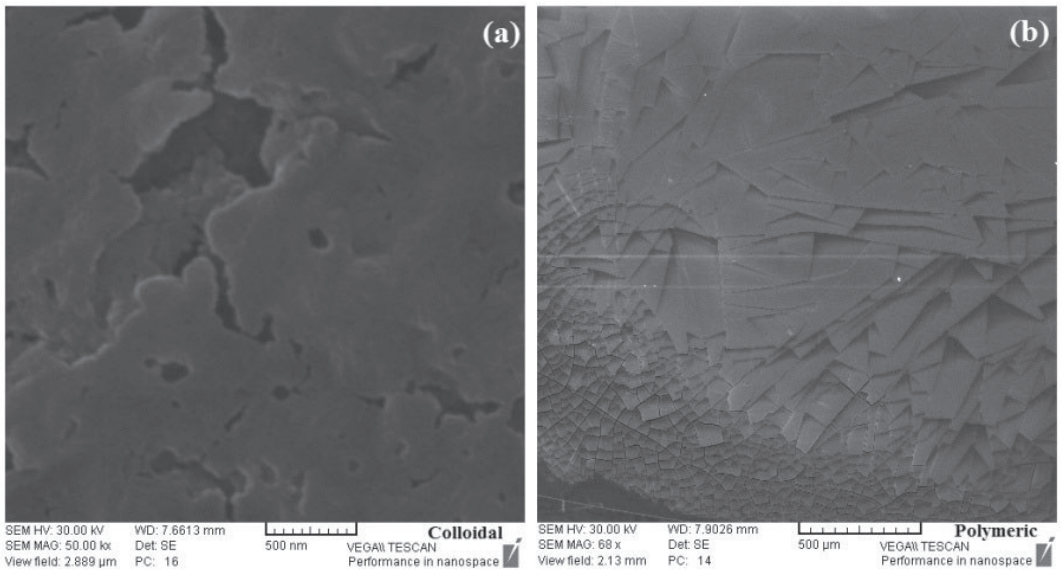

Fig. 8. SEM micrographs of the a) colloidal and b) polymeric sols after drying.

Downloaded from ijmse.iust.ac.ir at 5:31 IRDT on Sunday June 24th 2018

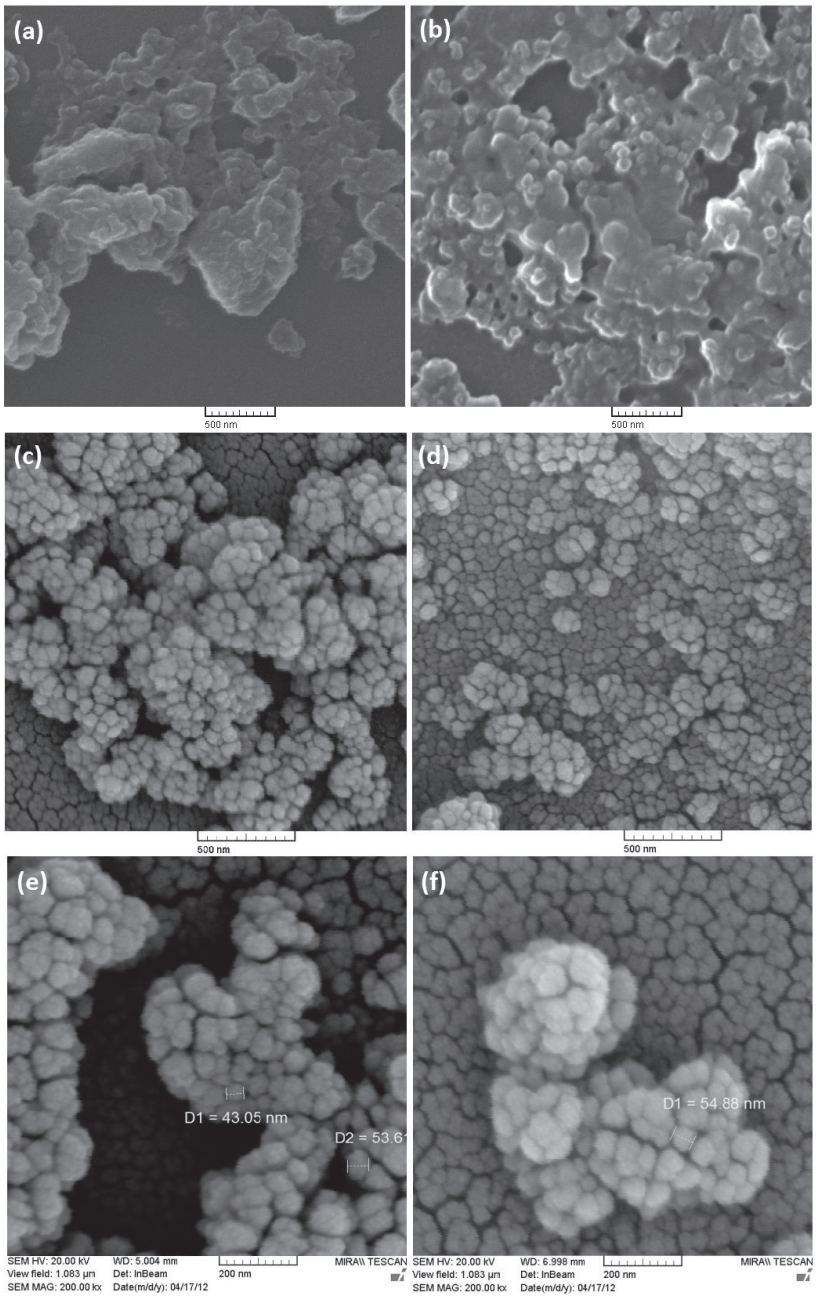

Fig. 8. SEM micrographs of the a) colloidal and b) polymeric sols after drying.

the colloidal sample are smaller than that of the polymeric one. The resultant spherical particles of colloidal and polymeric sols grow after calcination at 400 °C as are seen in Fig. 9(c,d). Also, according to Fig. 9(e,f), titania powders prepared by both routes after calcination are smaller than 60 nm.

Therefore, according to the images of FESEM, titania nanopowder can be produced by both colloidal and polymeric sol-gel routes.

CONCLUSIONS

In the present work, nanostuctured titania was synthesized by colloidal and polymeric sol-gel routes. Comparative study on these routes

Downloaded from ijmse.iust.ac.ir at 5:31 IRDT on Sunday June 24th 2018

showed that the polymeric titania sol is more stable than colloidal sol and the particle size of the polymeric sol is smaller than colloidal one (10-50 and 0.5-2 nm for the colloidal and polymeric sols, respectively). Thermogravimetery analysis of the prepared gels showed higher weight loss for polymeric sample that can promote crack formation in coatings prepared by the polymeric route. Phase analysis of the colloidal sample revealed anatase as the major phase at 400 °C and 550 °C converting to rutile at 650 °C, while the polymeric sample showed pure anatase phase up to 750 °C. On the basis of TG-DTA and XRD results, titania prepared by the polymeric route showed better thermal stability against phase transformation than that prepared by the colloidal route. Also, FESEM images showed that titania nanopowder can be produced by both sol-gel routes.

REFERENCES

1. Wu, S.Y., Lo, W. Ch., Chen, K. Ch., He, J. L., "Study on the preparation of nano-flaky anatase titania layer and their photovoltaic application", Curr. Appl. Phys. 10, 2010, S180-S183
2. Vaßen, R., Yi, Z., Kaßner, H., Stöver, D., "Suspension plasma spraying of TiO2 for the manufacture of photovoltaic cells." Surf. Coat. Technol., 203, 2009, 2146–2149
3. Phani, G., Tulloch, G., Vittorio, D., Skryabin, I., "Titania solar cells : new photovoltaic technology, Renewable Energy.", 22, 2001, 303-309
4. Chen X, X., Mao, S. S., "Titanium Dioxide Nanomaterials: Synthesis, Properties, Modifications, and Applications. Chem". Rev., 107, 2007, 2891-2959
5. López, A., Acosta, D., Martínez, A. I., Santiago, J., "Nanostructured low crystallized titanium dioxide thin films with good photocatalytic activity", Powder Technol., 202, 2010, 111–117
6. Choi, H., Stathatos, E., Dionysiou, D. D., "Photocatalytic TiO_2 films and membranes for the development of efficient wastewater treatment and reuse systems", Desalination, 202, 2007, 199–206
7. Campus, F., Bonhote, P., Gratzel, M., Heinen, S., Walder, L., "Electrochromic devices based on surface-modified nanocrystalline TiO_2 thin-film electrodes", Sol. Energy Mater. Sol. Cells, 56, 1999, 281-297
8. Manera, M. G., Cozzoli, P. D., Curri, M. L., Leo, G., Rella, R., Agostiano, A., Agostiano, A., Vasanelli, L., "TiO_2 nanocrystal films for sensing applications based on surface plasmon resonance", Synth. Met., 148, 2005, 25–29
9. Sekulić-Kuzmanović, J., "Mesoporous and Microporous Titania Membranes", PhD thesis, Twente University, 2004
10. Klein, L. C., "Sol-gel technology for thin films, fibers, performs", electronics, and specialty shapes, Noyes Publications, New Jersey, 1988
11. Sakka, S., "Handbook of sol-gel science and technology processing, characterization and applications", Kluwer academic publishers
12. Tsuru, T., "Nano/subnano-tuning of porous ceramic membranes for molecular separation", J. Sol-Gel Sci. Technol., 46, 2008, 349-361
13. Osada, Y., Nakagawa, T., "Membrane science and technology", Marcel Dekker, 1992
14. Bosc, F., Ayral, A., Albouy, P. A., Guizard, C., "A Simple Route for Low-Temperature Synthesis of Mesoporous and Nanocrystalline Anatase Thin Films", Chem. Mater., 15, 2003, 2463-2468
15. Mechiakh, R., Sedrine, N. B., Naceur, J. B., Chtourou, R., "Elaboration and characterization of nanocrystalline TiO_2 thin films prepared by sol-gel dip-coating", Surf. Coat. Technol., 206, 2011, 243-249
16. Sahni, S., Reddy, S. B., Murty, B. S., "Influence of process parameters on the synthesis of nano-titania by sol-gel route", Mater. Sci. Eng., A 452–453, 2007, 758–762
17. Li, B., Wang, X., Yan, M., Li, L., "Preparation and characterization of nano-TiO_2 powder", Mater. Chem. Phys., 78, 2002, 184–188
18. Venkatachalam, N., Palanichamy, M., Murugesan, V., "Sol-gel preparation and characterization of nanosize TiO_2: Its photocatalytic performance", Mater. Chem. Phys., 104, 2007, 454–459
19. Mao, L., Li, Q., Dang, H., Zhang, Z., "Synthesis of nanocrystalline TiO_2 with high photoactivity and large specific surface area by sol-gel method, Mater. Res. Bull.", 40, 2005, 201–208
20. Xinyan, X., Dongliang, L., Huiping, Z.,

Downloaded from ijmse.iust.ac.ir at 5:31 IRDT on Sunday June 24th 2018

Huanqin, C., "Synthesis of TiO_2 nano-particles and their photocatalytic activity for formaldehyde and methyl orange degradation", Front. Chem. Eng. China., 1(2), 2007, 178-183

21. Brinker, C. J., Scherer, G. W., "Sol-gel Science: The physics and chemistry of sol-gel processing. Hacourt brace Jovanovich", Boston, 1990
22. Sreethawong, T., Suzuki, Y., Yoshikawa, S., "Synthesis, characterization, and photocatalytic activity for hydrogen evolution of nanocrystalline mesoporous titania prepared by surfactant-assisted templating sol-gel process", J. Solid State Chem., 178, 2005, 329–338
23. Vargas, S., Arroyo, R., Haro, E., Rodriguez, R., "Effects of cationic dopants on the phase transition temperature of titania prepared by the sol-gel method", J. Mater. Res., 14, 1999, 3932-3937
24. Warrier, K. G. K., Kumar, S. R., Sibu, C. P., Werner, G., "High Temperature Stabilisation of Pores in Sol-Gel Titania in Presence of Silica", J. Porous Mater., 8, 2001, 311-317
25. Kreiter, R., Rietkerk, M. D. A., Bonekamp, B. C., Veen, H. M. V., Kessler, V. G., Vente, J. F., "Sol-gel routes for microporous zirconia and titania membranes", J. Sol-Gel Sci. Technol., 48, 2008, 203-211
26. Alem, A., Sarpoolaky, H., Keshmiri, M., "Sol-gel preparation of titania multilayer membrane for photocatalytic applications", Ceram. Int., 35, 2009, 1837-1843
27. Djaoued, Y., Badilescu, S., Ashrit, P. V., Bersani, D., Lottici, P. P., Robichaud, J., "Study of anatase to rutile phase transition in nanocrystalline titania films", J. Sol-Gel Sci. Technol., 24, 2002, 255-264
28. Zapalis, V. T., Praag, W. V., Keizer, K., Ross, J. R. H., Burggraaf, A. J., "Synthesis and characterization of primary alumina", titania and binary membranes, J. Mater. Sci., 27, 1992, 1023-1035
29. Alem, A., Sarpoolaky, H., Keshmiri, M., "Titania ultrafiltration membrane: Preparation, characterization and photocatalytic activity", J. Eur. Ceram. Soc., 29, 2009, 629-635
30. Mayadevi, S., Kulkarni, S. S., Patil, A. J., Shindeh, M. H., Potdar, H. S., Deshpande, S. B., Date, S. K., "Controlled chemical precipitation of titania for membrane applications—effect of heat treatment and fabrication conditions on its performance", J. Mater. Sci., 35, 2000, 3943-3949
31. Kermanpur, A., Ghassemali, E., Salemizadeh, S., "Synthesis and characterisation of microporous titania membranes by dip-coating of anodised alumina substrates using sol-gel method", J. Alloys Compd., 461, 2008, 331-335
32. Mozia, S., Morawski, A. W., Toyoda, M., Inagaki, M., "Application of anatase-phase TiO_2 for decomposition of azo dye in a photocatalytic membrane reactor", Desalination, 241, 2009, 97-105
33. Li, Z., Hou, B., Xu, Y., Wu, D., Sun, Y., Hu, W., Deng, F., "Comparative study of sol–gel-hydrothermal and sol–gel synthesis of titania-silica composite nanoparticles", J. Solid State Chem., 178, 2005, 1395-1405
34. Zhou, L., Yan, S., Tian, B., Zhang, J., Anpo, M., "Preparation of TiO_2-SiO_2 film with high photocatalytic activity on PET substrate", Mater. Lett., 60, 2006, 396-399
35. Song, C. F., Lu, M. K., Yang, P., Xu, D., Yuan, D. R., "Structure and photoluminescence properties of sol-gel TiO_2-SiO_2 films", Thin Solid Films, 413, 2002, 155-159
36. Kim, K. D., Bae, H. J., Kim, H. T., "Synthesis and characterization of titania-coated silica fine particles by semi-batch process", Colloids Surf., A 224, 2003, 119-126
37. Park, O. K., Kang, Y. S., "Preparation and characterization of silica-coated TiO_2 nanoparticle", Colloids Surf., A 257-258, 2005, 261-265
38. Shifu, Ch., Gengyu, C., "The effect of different preparation conditions on the photocatalytic activity of TiO_2-SiO_2/beads", Surf. Coat. Technol., 200, 2006, 3637-3643
39. Nielsen, A. E., "Crystal Growth, ed. H. S. Peiser", Pergamon Press, London, 1967
40. Jolivet, J. P., "Metal Oxide Chemistry and Synthesis: From Solution to Solid State", John Wiley & Sons, Chichester, 2000